Surface Energy Mapping of Kevlar® Fibers by Inverse Gas Chromatography

S. REBOUILLAT,[1] J. B. DONNET,[2] H. GUO,[2] T. K. WANG[2]

[1] Du Pont (UK) Limited, Maydown Research Centre, P.O. Box 15, Londonderry BT47 1TU, United Kingdom

[2] Laboratoire de Chimie Physique, Ecole Nationale Supérieure de Chimie de Mulhouse, 3 rue Alfred Werner, 68093 Mulhouse Cedex, France

Received 7 May 1997; accepted 18 June 1997

ABSTRACT: The surface energy characteristics of three Kevlar® fibers have been systematically studied using two inverse gas chromatography (IGC) techniques, i.e., at an infinite probe dilution and at a finite probe concentration, with the latter allowing a unique mapping of the surface energy levels, which complements greatly the more traditional characterization of the highest energy sites.

The standard thermodynamic parameters, such as the free energy $-\Delta G_A^\circ$, and the adsorption enthalpy and entropy (ΔH_A° and $-\Delta S_A^\circ$), as well as the dispersive and the specific component (γ_s^d and $\Delta G^{sp}/I^{sp}$) of the fiber surface energy, were determined from the retention behavior at zero coverage of selected molecules of various polarity. The γ_s^d values are between 49–58 mJ m^{-2} for the three fibers at 50°C. The polar components, ΔG^{sp} or I^{sp}, calculated by three different methods, reveal the polar feature of the fiber surface. It is interesting to note that the adsorption enthalpies ΔH_A° for the short chain alkane probes are nearly the same as their liquefaction energies.

Using the second IGC approach, i.e., at finite concentration, the isotherms for the adsorption of *n*-octane and *n*-hexylamine on the three selected Kevlar® fibers were constructed by the one-peak method. These are shown to be instrumental to establish the corresponding energy distribution functions. The results may indicate that, unlike the alkane probes, the polar molecules interact strongly with the Kevlar® fiber surfaces, which appear, in this case, energetically heterogeneous. The resulting energy distribution mapping opens new avenues towards the surface characterization of the global surface without the restriction of the averaging imposed by other bulk analysis techniques. J Appl Polym Sci **67:** 487–500, 1998

Key words: Kevlar® fibers; inverse gas chromatography; surface energy; adsorption isotherm; surface energy distribution and mapping

INTRODUCTION

It is well known that the poly(*p*-phenylene terephthalamide) (PPTA)–based fibers (Kevlar®) can be incorporated in a matrix of thermoplastic or thermoset polymer to formulate high-performance material composites. The ability of such advanced systems to use effectively the properties of Kevlar® fiber depend upon the strength translation at the interfacial zone, which is closely related to the surface energy distribution of the fiber and the matrix.[1] Therefore, the mapping of fiber surface energy and the fundamental understanding of the interaction phenomena involving fibers and polymer matrix is of great importance.

A number of methods have been developed to analyze the surface energy of fibers.[2–5] Among

Kevlar® is Du Pont's registered trademark.
Correspondence to: S. Rebouillat.

Journal of Applied Polymer Science, Vol. 67, 487–500 (1998)
 CCC 0021-8995/98/030487-14

those, the inverse gas chromatography (IGC) appears to be the currently preferred technique to measure the surface energy of fibers since it is a convenient, relatively simple, and flexible method.[6] However, the application of the IGC technique on the surface characterization of Kevlar® fibers has still been very limited. Less than 1% of the 800 papers published since the invention of IGC in 1967,[5] is dealing with PPTA fibers.[7–10] Moreover, most of these references do not address the characterization of a true bare fiber. In most cases, the selected Kevlar® fibers have been submitted to a surface stripping by solvent extraction.[7,8] Therefore, the purpose of the present work is to study systematically the surface energy of Kevlar® "ultraclean" fibers using the IGC techniques at the infinite probe dilution and at finite probe concentration. The latter may appear of great value when compared with the coupling of the calorimetry and gravimetry recently applied to Kevlar® fibers by Rebouillat et al.[10]

EXPERIMENTAL

The Principle of Inverse Gas Chromatography

IGC is simply an inversion of the conventional gas chromatography. Practically, a certain amount of fiber is used, as the stationary phase, to fill the column. After the column has been conditioned, several kinds of probe molecules (at infinite dilution or finite concentration) with known properties can be injected into it and carried through by helium. The key experimental parameter characterizing the equilibrium state of partitioning in the column is the net retention volume V_n, defined as the amount of carrier gas required to elute the injected probe molecules through the column. Thus, V_n is directly related to the gradient $\partial\Gamma/\partial c$ of the partition isotherm[11] by

$$V_n = A(1 - jY_0)\left(\frac{\partial\Gamma}{\partial c}\right)_P \qquad (1)$$

where Γ is the concentration of the probe on the solid surface, c is the concentration of the probe in the gas phase, P is the equilibrium pressure, A is the total surface area of the solid adsorbent in the column, Y_0 is the mole fraction of the probe in the gas phase at the column outlet, and j is the gas compressibility factor determined by

$$j = \frac{3}{2}\frac{(P_{in}/P_{out})^2 - 1}{(P_{in}/P_{out})^3 - 1} \qquad (2)$$

where, P_{in} is the pressure at the inlet of the column and P_{out} is the pressure at the outlet of the column.

Adsorption at Infinite Dilution

When adsorption takes place at infinite dilution, the interaction between the adsorbed probes is negligible, and Henry's law can be applied; i.e., the concentration of the probe on the solid surface is proportional to the equilibrium pressure. Thus, the term $\left(\frac{\partial\Gamma}{\partial c}\right)_p$ in eq. (1) becomes constant and equal to the surface partition coefficient K_s. In this case, the Vn is practically independent of the probe concentration.[5,12–13]

Determination of Standard Thermodynamic Parameters

At infinite dilution, several standard thermonamic parameters, such as thedy free energy ΔG_A°, the enthalpy ΔH_A°, and the entropy ΔS_A° of adsorption, can be determined according to Katz and Gray.[13]

The standard free energy of transferring one mole of probe from the standard gaseous state to a standard adsorption state is related to Vn as follows:

$$\Delta G_A^\circ = -\mathrm{R}T\ \mathrm{Ln}\ V_n + \mathrm{B} \qquad (3)$$

where T is the column temperature (in °K), R is the gas constant, and B is a constant depending on the reference state and on the total surface area of the fiber in the column. B is expressed by

$$\mathrm{B} = -\mathrm{R}T\ \mathrm{Ln}\left(\frac{P^\circ}{\pi^\circ Sg}\right) \qquad (4)$$

where S is the specific surface area, and g is the fiber weight in the column. When the mean distances between the probe molecules in the vapor phase is equal to the spans between the adsorbed one at the solid surface, i.e., the De Boer's reference state, the spreading pressure π° has a value 0.338 mN m at P° = 101.3 kPa (1 atm) and 0°C.[14] By measuring the retention volume at different temperature, the enthalpy of adsorption ΔH_A° can be deduced from

$$\Delta H_A^\circ = -\mathrm{R} \cdot d(\mathrm{Ln}\ Vn)/d(1/T) \qquad (5)$$

From eq. (5), one can see that the ΔH_A is now independent of the reference state. The adsorption entropy ΔS° is obtained directly from the classic equation

$$\Delta S_A^\circ = (\Delta H_A^\circ - \Delta G_A^\circ)/T \qquad (6)$$

Determination of Dispersion Energy Component γ_s^d

The adsorbed probe molecules may exchange different types of interactions with the solid surface. Generally, the surface energy γ_s can be is split into the following two parts: dispersive γ_s^d and specific γ_s^{sp} energy components,

$$\gamma_s = \gamma_s^d + \gamma_s^{sp} \qquad (7)$$

In practice, *n*-alkanes are used to obtain the dispersive component.

As a first approximation, the free energy of adsorption ΔG^0 can be linked with the work of adhesion W_A between the vapor probe (adsorbate) and the solid stationary phase (adsorbent) per unit surface area, as follows:

$$-\Delta G_A^\circ = NaW_A \qquad (8)$$

where N is the Avogadro's number, and a is the surface area of an adsorbed probe molecule.

When nonpolar probes like *n*-alkanes are employed as adsorbates, the work of adhesion is dominated by dispersive interactions at the interface[15]; thus, the IGC measurement yields the dispersive component of the surface free energy, γ_s^d, from

$$W_A = 2(\gamma_s^d \gamma_L^d)^{1/2} \qquad (9)$$

Two approaches have been used to access the γ_s^d value of the solid stationary phase.

(1) From the free energy of adsorption $\Delta G_{\mathrm{CH_2}}$ of a methylene (—$\mathrm{CH_2}$—) group in the alkane series ($\mathrm{C}_n\mathrm{H}_{2n+2}$), Dorris and Gray[16] determined the γ_s^d as follows:

$$\gamma_s^d = \frac{\Delta G_{\mathrm{CH_2}}^2}{4N^2 a_{\mathrm{CH_2}}^2 \gamma_{\mathrm{CH_2}}} \qquad (10)$$

where $a_{\mathrm{CH_2}}$ is the area covered by a methylene group (0.06 nm^2), and $\gamma_{\mathrm{CH_2}}$ is the surface energy of a methylene group (37.5 mJ m^2).[16,17] This approach has been widely accepted and used for the determination of γ_s^d value which, in practice, is simply derived from the slope of the linear plot of ΔG^0 of a series of *n*-alkanes versus their carbon atom numbers.

(2) The dispersive component γ_s^d can also be determined[18] from the surface area of the alkane molecules, a, and their dispersive component γ_L^d. The combination of the eqs. (3), (8), and (9) gives directly

$$\mathrm{RT\ ln}\ Vn = 2N(\gamma_s^d)^{1/2} a(\gamma_L^d)^{1/2} + C^{st} \qquad (11)$$

By plotting RT ln Vn of alkane probes versus $a(\gamma_L^d)^{1/2}$, the γ_s^d can be obtained directly from the slope of the straight line. The $a(\gamma_L^d)^{1/2}$ values for some alkanes can be found in the literature.[5,18]

Figure 1(a) and (b) illustrate these two approaches for the determination of the dispersive component γ_s^d. γ_s^d can be calculated from the slope in Figure 1(a) according to eq. (10) and from that in Figure 1(b) according to eq. (11).

Determination of Specific Interaction Energy with Polar Probes

When polar adsorbates are used in the IGC experiment, then both dispersive and specific interactions take place between the adsorbate and the adsorbent. Theoretically, the specific component can be obtained by assuming that (1) *n*-alkanes exchange only dispersive interactions, and (2) the dispersive and the polar components of the surface energy are additive.

Several methods have been developed for these determinations. The common point between them is to take the *n*-alkanes as the reference for the strictly dispersive interactions with the solid surface and then to deduce the nondispersive contribution from the distance to the alkane reference line, as illustrated in Figure 1(b)–(d).

The key differences between the methods, proposed so far to determine the various energy components, lie in the definition of the discerning criteria to separate the dispersive contribution from the total interaction energy in order to obtain by subtraction the specific component. Three techniques are illustrated below.

(1) *Probe surface area method.* In characteriz-

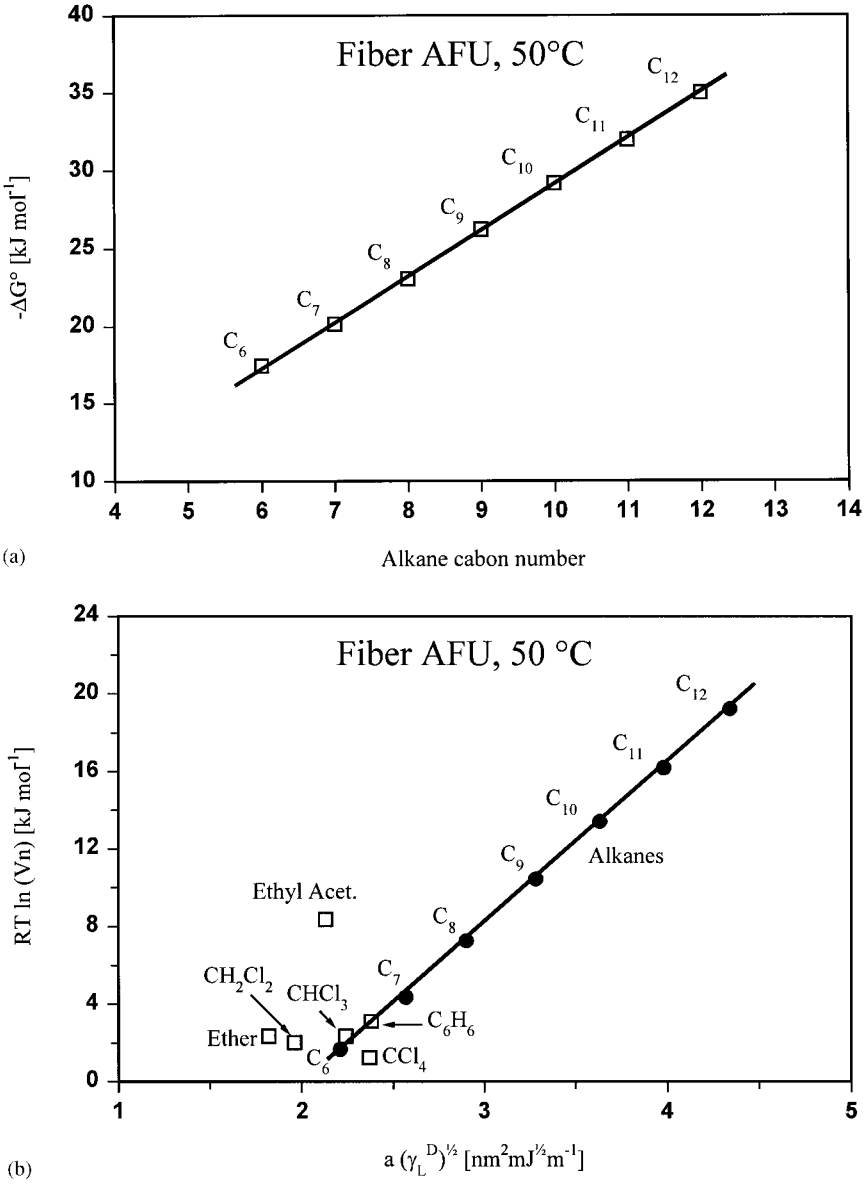

Figure 1 (a) The adsorption energy of a series of alkane probes on fiber AFU versus the carbon number at 50°C, from the slope of the straight line the dispersive surface energy component of the fiber γ_s^d, can be deduced according to eq. (10). (b) $RT \ln(Vn)$ versus $a(\gamma_L^d)^{1/2}$ plot from the slope the γ_s^d can also be deduced according to eq. (11); ΔG^{sp} for the polar probes is equal to the vertical distance between the data points and the alkane reference line. (c) The adsorption energy of a series of polar probes on fiber AFU versus the probe surface area at 50°C; ΔG^{sp} is defined in a similar way as in (b); the specific surface energy component of the fiber I^{sp} can be deduced according to eq. (13). (d) The adsorption energy of a series of polar probes on fiber AFU versus the probe polarizability at 50°C; ΔG^{sp} can also be calculated similarly.

ing several solids, such as carbon black, silica, and carbon fiber, Wang et al.[12] have proposed a simplified criterion using only the surface area of the probe molecules. The latter can be calculated from the liquid density according to the spherical[19] or the cylindrical[20] models.

As shown on Figure 1(c), plotting the free energy of adsorption as a function of the surface area of the selected probe mole-

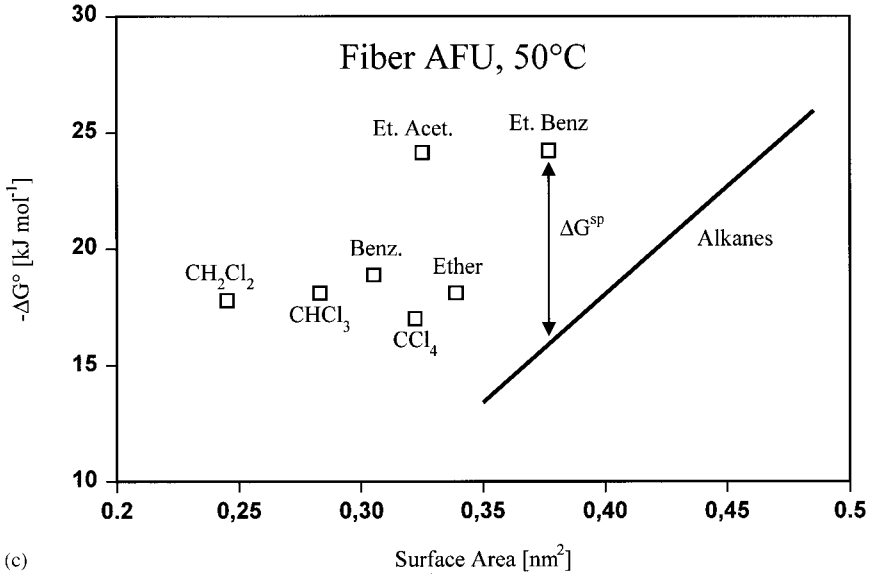

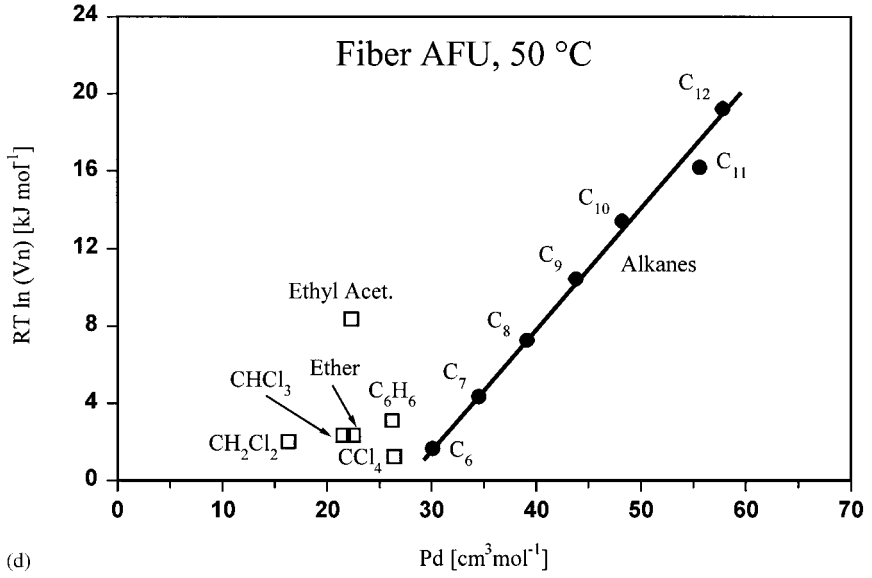

Figure 1 *(Continued from the previous page)*

cules, provides access to the specific free energy ΔG^{sp} through the following equation:

$$\Delta G_A^{sp} = (-\Delta G_A^{\circ}) - (-\Delta G_{A,\text{alkane}}^{\circ}) \quad (12)$$

A specific interaction parameter I^{sp} can then be defined[12] as

$$I^{sp} = \frac{\Delta G_A^{sp}}{Na_p} \quad (13)$$

where a_p is the surface area occupied by the polar probe. I^{sp} has the same dimension as the dispersive component γ_s^d, thus allowing a direct comparison.

This method appears to be a simplified version of the following approach.

(2) $a(\gamma_L^d)^{1/2}$ *term method*. A different way[18] of calculating ΔG^{sp} is used by taking into account not only the surface area a but also the dispersive component γ_L^d of the probes. γ_L^d is determined from the contact angle on a reference solid, and the term $a(\gamma_L^d)^{1/2}$ for each probe is the variable for the plot shown in Figure 1(b).

(3) *Polarizability Method*. Another alternative method, proposed by Dong et al.,[21] takes

Table I Parameters Used for the Determination of Specific Interactions

Probe	Surface Area[a] (nm^2)	P_d[b] (cm^3 mol)	$a(\gamma_L^D)^{1/2}$ [c] (nm^{+2} $mJ^{+1/2}$ m^{-1})
Hexane	0.39	30.1	2.21
Heptane	0.43	34.5	2.57
Octane	0.46	39.1	2.90
Nonane	0.49	43.8	3.28
Decane	0.52[d]	48.2	3.63[d]
Benzene	0.31	26.2	2.38
THF	0.29	19.9	2.13
Acetone	0.27	16.2	1.73
EtAc	0.33	22.3	2.13
Ether	0.34	22.5	1.82
CH_2Cl_2	0.25	16.3	—
$CHCl_3$	0.28	21.5	2.20
CCl_4	0.32	26.4	2.38

[a] From Donnet et al.[20]
[b] From Dong et al.[21]
[c] From Lloyd et al.[5] and Schultz et al.[18]
[d] Extrapolated values.

the molecular polarity of the probes into consideration. The deformation polarization parameter P_d was used instead of the surface area a and the term $a(\gamma_L^d)^{1/2}$. P_d is obtainable from the macroscopic refraction index measurement according to

$$P_d = R_M = \frac{n^2 - 1}{n^2 + 2}\frac{M}{\rho} \qquad (14)$$

where R_M is the molecular refraction, n is the refraction index, and M and ρ are the molecular weight and the density of a given probe. Figure 1(d) shows an example illustrating this method.

Table I provides the parameters used for the three methods.

It should be stressed that if the solid surface is heterogeneous in terms of energy distribution, the results obtained with the infinite dilution technique will be mostly influenced by the highest energy sites. Therefore, the infinite probe dilution technique cannot solely provide a complete surface energy mapping of the considered stationary phase.

Adsorption at Finite Concentration

Unlike the infinite dilution method, the adsorption at finite concentration consists in injecting gradual amounts of liquid probes. The analysis of the chromatographic peaks, for example, Figure 2, allows an assessment of the various energy levels for different surface coverage ratio.

Adsorption Isotherm

The adsorption isotherm provides the amount of probe adsorbed for a given equilibrium pressure. Basically, using IGC, the isotherm is drawn from a series of chromatograms (see main peak and experimental peaks in Fig. 2) obtained for gradual injections of the selected probe. This procedure is known as the multi-injection method.[11] This time-consuming approach can be simplified if the one peak method[11] requirements are met. In this case, only the main peak, as provided in Figure 2, has to be used to construct the adsorption isotherm. Some precautions must be taken prior to considering the application of the one peak method, as follows: (1) the detector response must be linear, and (2) a series of chromatographic peaks corresponding to a series of step-by-step increasing injections must superpose on the diffusion side, i.e., the tail of the peak (Fig. 2). This situation corresponds to the most frequently encountered isotherm type II but cannot be considered as universal; therefore, it is important to validate the related assumptions. In this case only, the main peak can be regarded as the superposition of peaks comparable to the one obtainable by the multi-injection method; therefore, it can be fragmented in as a series of individual curves corresponding to various injection volumes. In practice, the descending part of the main chromatographic peak can be numerically divided into theoretical curves (see the hypothetical peaks in Fig. 2) for

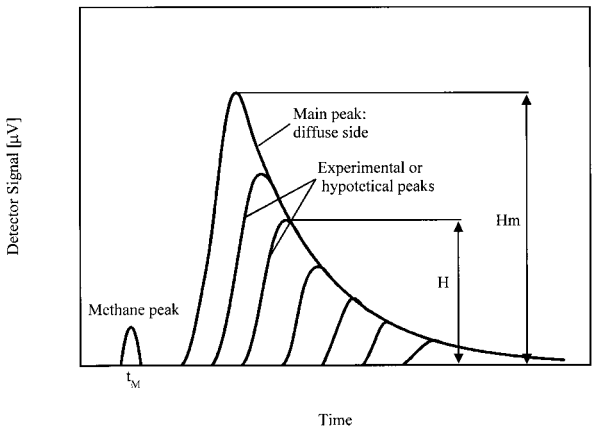

Figure 2 Illustration of an IGC chromatographic peak at finite dilution.

analysis.[22] For each curve corresponding to a given retention volume V_n, the partial pressure of the adsorbate P and the adsorbed quantity Q can be obtained from the following equations derived from the mass balance:

$$P = \frac{RT \cdot W_p \cdot H}{F' \cdot S_p} \quad (15)$$

$$Q = \frac{W_p \cdot S_{ads}}{W_s \cdot S_p} \quad (16)$$

where W_p is the quantity of probe injected (mole), H is the height of the chromatographic peak, F' is the corrected flow rate of the carrier gas, S_p is the area of the chromatographic peak, W_s is the mass of the stationary phase, and S_{ads} is the adsorption area[23] of the considered chromatographic peak.

Energy Site Distribution

The nonaxysymmetrical shape of the chromatographic peaks or the retention time variation with the injected volume (Fig. 2) have been observed on nonporous solids and interpreted as an indication of the surface energy heterogeneity.[24,25] Theoretically, this heterogeneity can be described[24,25] by a distribution function $\chi(\varepsilon)$ of the surface sites, corresponding to the energy level ε, which interact with the adsorbed probe molecules. This function, defined by Rudzinski et al.,[24] is related to the experimental adsorption isotherm by the following expression:

$$N(P, T) = N_0 \int_0^{+\infty} \chi(\varepsilon), \theta(\varepsilon, P, T)\, d\varepsilon \quad (17)$$

where $N(P, T)$ and N_0 are the global number of molecules adsorbed at saturation pressure P and temperature T. $\theta(\varepsilon, P, T)$ is the local, specific isotherm corresponding to the number of molecules involving an adsorption energy ε. There is no direct analytical solution for this expression. Various reduced mathematical treatments, such as the Fourier transform, were developed to circumvent this problem and are also described by Rudzinsky et al.[24]

In this article, we have adopted Robson's Model,[22,25,26] which involves the local adsorption isotherm by deriving the function $\chi(\varepsilon)$ from eq. (1). This gives the following expressions:

Table II Characteristics of the Columns Packed with Kevlar® Fibers

Fibers	AFK	AFU	AFV
Linear density (g m^{-1})	0.093	0.316	0.330
Filaments per fiber (−)	570	1333	1333
Filament diameter (μm)	12	15	15
Strength (GPa)	3.345	2.790	2.915
Modulus (GPa)	93.65	112.62	69.92
Column packing			
Sample weight (g)	3.89	4.63	5.14
Surface area (m^2)	0.91	0.86	0.96

$$\chi(\varepsilon) = -\left(\frac{P}{RT}\right)^2 \frac{\partial V_n(P, T)}{\partial P} \quad (18)$$

$$\varepsilon = -RT \ln \frac{P}{K} \quad (19)$$

where K (in mm Hg) is the preexponential factor of Henry's constant. K is related to the molecular weight of the probe M and the experimental temperature T by $K = 1.76 \cdot 10^4 \sqrt{MT}$. The $\chi(\varepsilon)$ function was solved numerically from the global adsorption isotherm. The adequate corrections, to consider only the first monolayered molecules that interact with the solid, need to be taken into account as per the traditional computing of isotherms.

Experimental Procedures

Samples of three modified Kevlar® fibers, coded AFK, AFU, and AFV, were used as received from Du Pont Ltd. (U.K.). AFK and AFV are untreated Kevlar®-29 samples with different filament diameters (12 μm for AFK and 15 μm for AFV). AFU is a Kevlar®-49 high modulus sample already annealed (filament diameter 15 μm). The samples were specially engineered to obtain an ultraclean bare surface, free of any processing finish, and conditioned to avoid contamination or abnormal oxidation. The properties of these fibers, reported in Table II, have been measured as per the corresponding ASTM procedures.

Throughout this work, a typical stainless steel column with a length of 60 cm and a diameter of 4.4 mm was used. Before packing, the columns were treated with a 10% nitric acid solution for 30 min, then washed with distilled water and acetone and dried overnight in an oven at 120°C. Approximately 4–5 g of Kevlar® fibers, previously

cut into 50 cm long pieces and partially fibrillated, was filled in each column. The characteristics of each column used in this work are also given in Table II.

The packed column was then mounted on an Intersmat IGC 121DFL gas chromatography equipped with a hydrogen flame ionization detector (FID). Prior to any measurement, the column was conditioned for 12 h by allowing through it a helium stream at 180°C in order to remove the adsorbed impurities and the residual water. The measurements were then performed on the same column in the temperature range of 40 to 70°C for the infinite dilution measurements and at 46°C for the finite concentration ones.

The helium was used as a carrier gas at a flow rate of 25 mL min determined by the theoretical plate number.[11] Flow rates were measured at the column end using a soap bubble flow meter and then corrected for the temperature of the gas in the flow meter, the water vapor pressure, and the pressure drop in the column.

For the test at infinite probe dilution, both nonpolar (*n*-alkanes) and polar probes were used for the analysis. All probes were chromatographic-grade chemical products obtained from Aldrich. To measure the retention time of probes, a small amount of vapor was taken from the headspace of the liquid probes and injected into the chromatographic column along with the methane as a marker. The vapor volume of the probe injected was as small as possible so as to satisfy the condition of adsorption at infinite dilution, which corresponds to a zero coverage of the surface.

For the test at finite concentration, *n*-octane (the nonpolar probe) and *n*-hexylamine (the polar probe) were used. The liquid volume of the injected probe, taken with a 1 or 5 μL Hamilton syringes, was in the range of 0.5 to 2 μL in order to obtain the adsorption isotherms over a sufficiently wide range of equilibrium pressures. The one peak method was used for the determination of the function $\chi(\varepsilon)$. Precautions were taken to check the superposition of the diffuse descending sides (see Fig. 2) of the chromatographic peaks. For the Kevlar® fibers tested, excellent superposition was evidenced for the two probes tested.

RESULTS AND DISCUSSION

Results from the Adsorption at Infinite Dilution

As a preliminary check, the retention volumes of the alkanes from *n*-butane to *n*-dodecane have been measured using the fiber sample AFU. Under the experimental conditions, the retention volume of the *n*-alkanes with low carbon numbers, like *n*-butane (C4) and *n*-pentane (C5), is nearly the same as the methane marker. In this case, the measured standard free energy ΔG° of adsorption is meaningless. Therefore, in the present study, the probes used to evaluate the dispersive component of the surface energy of Kevlar® fibers were *n*-alkanes ranging from *n*-hexane to *n*-dodecane, preferably from *n*-heptane to *n*-decane.

Determination of the Thermodynamic Parameter Using the Alkanes

Within the range of temperatures considered in this study (40–70°C), the plots of $\mathrm{Ln}(V_n)$ versus $1/T$ for all alkane probes on Kevlar® fibers are linear. As an example, a typical plot of the adsorption of the *n*-alkanes on the fiber AFU is shown in Figure 3. The enthalpy of adsorption ΔH_A° was determined for each probe from the slope corresponding to the eq. (5). These results are listed in Table III with the extrapolated values for *n*-undecane and *n*-dodecane. For the same fiber, the ΔH_A value increases with increasing molecular sizes (from *n*-heptane to *n*-decane). This is in agreement with the results obtained by other workers.[7,8] It appears from Table III that the enthalpies of adsorption ΔH_A° for alkanes are nearly of the same levels as the enthalpy of liquefaction $-\Delta H_L$, at least for smaller alkanes, such as *n*-heptane and *n*-octane. It means that mainly, and possibly only, the Van der Waals interactions are determinant in the interactions between the alkane molecules and the Kevlar® fiber surface. However, the difference becomes appreciable with the larger alkanes. This is consistent with the observations by Rebouillat et al.[9] on a Kevlar® 29 fiber with *n*-dodecane. The enthalpy of adsorption has been measured on an untreated Kevlar® 29 fiber[10] using aniline and epoxystyrene as polar probes. They found that the ΔH_A for the two probes can be higher (aniline) or lower (epoxystyrene) than their respective liquefaction enthalpy. Moreover, the ΔH_A° increases also with the "cleanness" of the Kevlar® fibers according to the study conducted in Chappell and Williams.[8] The samples, used for this work, are ultraclean fibers free of any surface coating and not submitted to any solvent extraction. In comparison with the results given in Chappell and Williams,[8] the values of about 41.4–43.7 kJ mol^{-1} for *n*-octane are larger that the as-received and *n*-hexane extracted com-

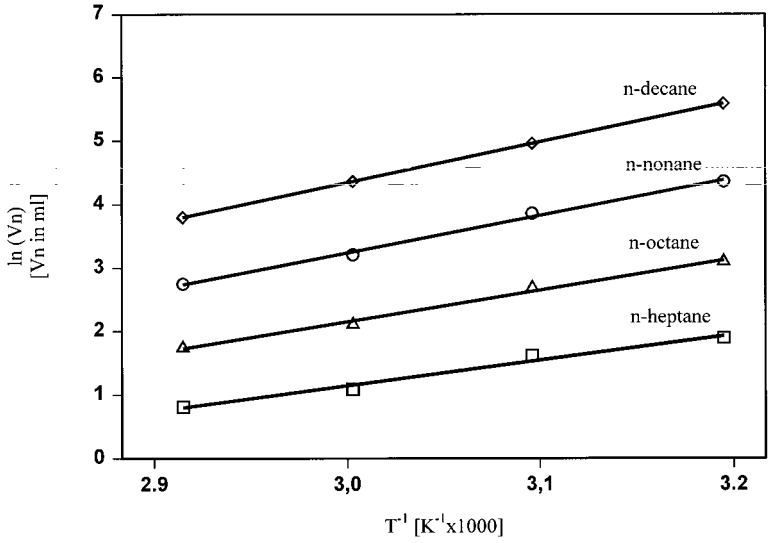

Figure 3 Variation of $\mathrm{Ln}(V_n)$ as a function of $1/T$ for the adsorption of the n-alkanes on the fiber AFU.

mercial Kevlar® 49 fibers used in the work of cited. Nonetheless, our values are still smaller than those obtained for the fibers treated via polar solvent extraction, such as water and acetone.[8] It is worthwhile to mention that in such an extraction, water could change either the surface crystalline structure[27] or the surface chemical composition by affecting the H-bonding patterns and the molecule diffusion in the intercrystalline slits and in the amorphous zones.[10] It remains to be clarified whether the ΔH_A provided in Chappell and Williams[8] can really be compared directly with our results.

The ΔG_A° and ΔS_A°, calculated according eqs. (3) and (6), are listed in Table IV. They are all dependent on the length of the alkane molecules. The ΔG_A° is not very sensitive to the surface cleanness of the fibers according to Chappell and Williams.[8] Therefore, it is not surprising to observe that the values obtained for the fiber samples considered here are essentially of the same order of magnitude than the one reported previously.[8] Typically, 21.38–23.05 kJ mol^{-1} compared to 19.8–23.4 kJ mol^{-1} for the n-octane at 50°C cannot be considered as statistically different. However, as is the enthalpy, the entropy of adsorption is sensitive to the surface energy state.[8] The previous observations made for the ΔH_A values extend to the ΔS_A° range (57.07–61.60 J $\mathrm{mol}^{-1}\mathrm{K}^{-1}$) obtained here versus the series of Kevlar® fibers with different treatment conditions considered in Chappell and Williams.[8]

Table III The Enthalpy of Adsorption ΔH_A° (kJ mol) of the n-Alkane Probes on Kevlar®

Probes	AFK	AFV	AFU	ΔH_L[a]
n-Heptane	36.4	38.9	33.5	36.9
n-Octane	41.4	43.7	41.6	41.8
n-Nonane	47.3	50.2	48.7	46.8
n-Decane	53.4	57.2	53.5	51.8
n-Undecane[b]	58.9	62.9	61.1	56.8
n-Dodecane[b]	64.5	69.0	67.8	61.7

[a] ΔH_L is defined as the liquefaction energy of the probe molecules; the values listed here were quoted from Katz and Gray.[13]
[b] Extrapolated values.

Determination of the Dispersive Component γ_s^d

Figure 1 provides several examples of plots from which the γ_s^d and the ΔG^{sp} are calculated. In Figure 1(a), the standard adsorption energy $-\Delta G_A^\circ$ versus the carbon number of the alkanes is plotted. The slope of the straight line gives the $\Delta G_{\mathrm{CH_2}}$ from which the γ_s^d is obtained according to eq. (10). Alternatively, in applying eq. (11), the γ_s^d can also be deduced from the slope of the straight line in Figure 1(b). The difference between the values on the vertical axes in Figure 1(a) and (b) is the constant B of eq. (4). In the experimental conditions, (T = 50°C, $Sg \sim 1\ \mathrm{m}^2$), B is about 16 kJ mol^{-1}.

The results of the γ_s^d values and their temperature dependence for the three fibers are compared

Table IV Free Energy, $-\Delta G_A^\circ$ (kJ mol), and Entropy, $-\Delta S_A^\circ$ (J mol K^{-1}), of Alkane Adsorption on the Three Fibers at 50°C

n-Alkane Probes	$-\Delta G_A^\circ$ (kJ mol)			$-\Delta S_A^\circ$ (J mol K^{-1})		
	AFK	AFV	AFU	AFK	AFV	AFU
Heptane	18.57	19.78	20.13	54.87	59.19	41.13
Octane	21.38	22.90	23.05	61.60	64.41	57.07
Nonane	24.48	26.14	26.22	70.23	74.48	63.32
Decane	27.57	29.39	29.19	79.49	86.09	74.79

in Table V. The two methods give consistent results. Among the two low modulus, i.e., unannealed AFK and AFV Kevlar® 29 samples, the latter shows a higher γ_s^d. Is it due to the fiber diameter difference or is it caused by other factors? The question remains open for further investigation. Nonetheless, it is conceivable at this stage to consider that, during manufacturing, the fiber heat drying has more effect on the surface structural changes[9,28] for the smaller diameter and the much lower linear density fiber AFK. Furthermore, the intermediate modulus value of AFK, provided in Table II, may justify this interpretation in terms of a preannealing, which, for our study, would position sample AFK more in between the two others than at the lower end. As to the annealed AFU, the γ_s^d level is virtually the same as the AFK. This series of γ_s^d values are also higher than the reported ones[10] where, however, the column preconditioning is very different. It is reported in Chappell and Williams[8] that γ_s^d depends strongly on the surface cleanness of the Kevlar® fibers, from 32 mJ m^{-2} for a finished fiber to 65 mJ m^{-2} for an acetone extracted one. The higher γ_s^d values between 49–58 mJ m^{-2} for the fibers in this study can be attributed at least partly to the surface ultraclean state. From Table V, we see also clearly that γ_s^d decreases when rising the column temperature; this behavior was also observed on carbon fiber.[23]

Table V Dispersive Component γ_s^d of the Surface Energy for Kevlar® Fibers at 50°C and Its Temperature Dependence, Deduced from Two Different Methods

Fibers	AFK	AFV	AFU
γ_s^d (mJ m^{-2})[a]	51	58	52
$-d\gamma_s^d/dT$ (mJ m^{-2} K^{-1})[a]	0.19	0.22	0.30
γ_s^d (mJ m^{-2})[b]	49	56	50
$-d\gamma_s^d/dT$ (mJ m^{-2} K^{-1})[b]	0.25	0.30	0.34

[a] Calculated with eq. (10).
[b] Calculated with eq. (11).

Polar Components of the Adsorption Energy

On the typical diagrams in Figure 1(b)–(d), the specific component ΔG^{sp} was calculated from the difference on the vertical y-axis between the considered polar probe position and the alkane reference line, as illustrated on Figure 1(c).

The three methods previously described under the Experimental Section, entitled "Adsorption at Infinite Dilution," were used for the assessment of the specific components. Table I presents the parameters adopted, and the results are gathered in Tables VI–VIII.

The specific interaction parameter I^{sp}, defined in eq. (13), can be used to estimate the relative importance of polar contribution compared to the dispersive one. In Table VI, it appears that the ether has a much weaker polar interaction ($\sim$ 30 mJ m^{-2}) with the fiber surface than dichloromethane ($\sim$ 100 mJ m^{-2}), while the dispersive component has a value of about 50 mJ m^{-2}. Based on the surface areas of the probes [Fig. 1(c)], the ΔG^{sp} calculated according to eq. (12) can be compared with the one obtained by the other methods. Ethyl acetate and dichloromethane exhibit stronger specific interactions than other polar probes.

The method using, as a criterion, the term $a(\gamma_L^d)^{1/2}$ [Fig. 1(b)] gives different numerical values. Only the ethyl acetate has a much higher polar contribution than the other probes (Table VII). In Figure 1(b), the data for the tetrachlorocarbon drops below the reference line; this is not an unusual, but a difficult, aspect to explain. It is interesting to compare the ΔG^{sp} values for the three fibers of this study with a commercial Kevlar® K29 fiber,[29] which has been exposed to a solvent extraction with trichloroethane (Table

Table VI The Specific Interaction Parameter I^{sp} (mJ m^{-2}) and Energy $-\Delta G^{sp}$ (kJ mol^{-1}) of the Polar Probes on Kevlar® Fibers at 50°C Calculated According to the Probe Surface Area Criterion

	AFK		AFV		AFU	
Polar Probes	I^{sp}	$-\Delta G^{sp}$	I^{sp}	$-\Delta G^{sp}$	I^{sp}	$-\Delta G^{sp}$
Benzene	50.3	9.24	62.0	11.39	56.6	10.40
Et. Benzene	36.6	8.31	41.7	9.48	38.3	8.69
Et. Acetate	68.0	13.3	85.0	16.64	69.9	13.69
Ether	28.1	5.73	37.9	7.74	30.8	6.29
CH_2Cl_2	93.4	13.78	112.6	16.62	102.9	15.18
$CHCl_3$	63.5	10.82	77.5	13.21	69.1	11.77
CCl_4	31.9	6.18	38.4	7.45	35.4	6.86

VII). The latter was also heated at 180°C during a column preconditioning comparable to the one in the present work. All the ΔG^{sp} data in Table VII were obtained with the same calculation method. It is worthwhile to notice the excellent correlation between the ultraclean fibers and the purified commercial one. This tends to validate the extraction method used by the fiber supplier compared to the lab procedures used in previous studies.[8]

The ΔG^{sp} results obtained with the polarizability method are presented in Table VIII. Although the absolute numerical values are different, the relative classification of the polar probe interactions with the fiber samples is similar to the one observed via the surface area method (Table VI). In this case, all the data are located above the reference alkane line, as shown in Figure 1(c) and (d). The polarization method might be revealed to be a more universal approach.

The three methods bring the following overlapping conclusions:

(1) the ethyl acetate always has a strong interaction with the Kevlar® surface probably through the ester function,
(2) the three methane chlorides present similar behavior, i.e., the specific interaction decreases with the increasing chlorine number in methane; and
(3) benzene and ether present a medium level of interaction through the polarisable π-bonds or —O— function.

This series of results shows the polar feature of the Kevlar® fiber surface and confirms the observation with aniline and epoxystyrene probes obtained from the same kind of fiber.[10]

From an experimental point of view, it should be stressed that the retention volume in the IGC measurement conditions, despite a flow rate of the carrier gas of 25 mL min^{-1} and $\sim$ 1 m^2 of total fiber surface area available in the columns, might be too small for an accurate surface scanning with some polar probes. It might be advisable to use larger size polar probes, although the critical pore size and the potential diffusion effects described

Table VII The Specific Interaction ΔG^{sp} (kJ mol^{-1}) of the Polar Probes on Kevlar® Fibers at 50°C Calculated According to the Criterion of $a(\gamma_L^d)^{1/2}$ Term

Probes	AFK	AFV	AFU	K29[a]
Benzene	0.17	0.08	0.32	—
Et. Acetate	8.20	9.77	7.75	7.45
Ether	4.45	5.11	4.31	3.24
CH_2Cl_2	2.78	2.64	2.80	1.89
$CHCl_3$	0.93	0.80	0.74	0.27

[a] K29 is a commercial fiber after extraction with trichloroethane and treated at 180°C.[29]

Table VIII The Specific Interaction Energy ΔG^{sp} (kJ mol^{-1}) of the Polar Probes on Kevlar® Fibers at 50°C Calculated According to the Probe Polarizability Criterion

Probes	AFK	AFV	AFU
Benzene	4.09	5.29	4.31
Et. Acetate	12.55	15.65	12.15
Ether	6.11	6.88	5.98
CH_2Cl_2	9.69	10.01	9.77
$CHCl_3$	6.76	7.04	6.64
CCl_4	2.45	2.03	2.30

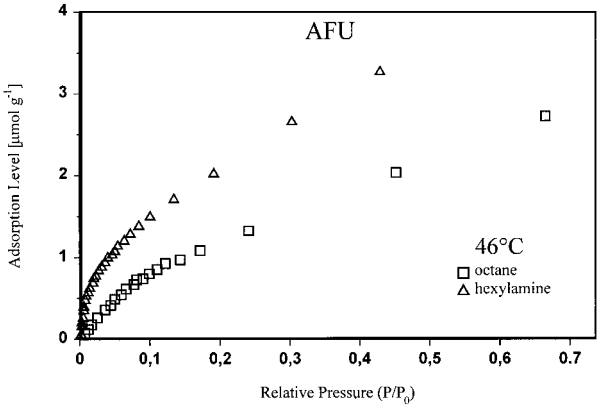

Figure 4 Adsorption isotherms of *n*-octane and *n*-hexylamine on the fiber AFU at 46°C.

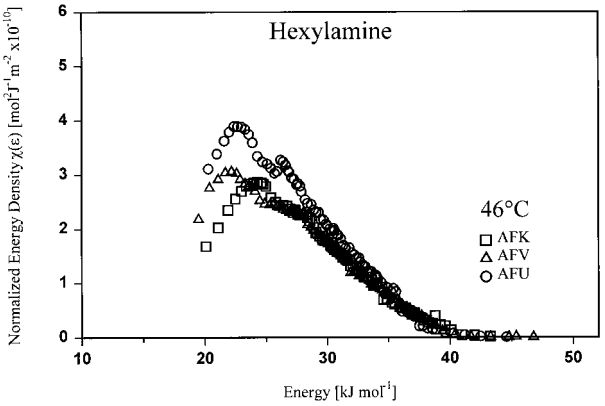

Figure 6 Energy distribution functions of the *n*-hexylamine adsorption on Kevlar® fibers at 46°C.

in[9–10] may have never been discovered without involving these conditions.

Results from the Adsorption at Finite Concentration

Isotherms for the adsorption of *n*-octane and *n*-hexylamine on Kevlar® fibers are computerized from eqs. (15) and (16). A typical example is shown in Figure 4 for the fiber AFU. Here, the isotherms are plotted as the adsorption amount against the relative pressure P/P_0; P_0 is the saturation pressure at the measurement temperature. It is clear that the adsorption amount of *n*-hexylamine is higher than that of *n*-octane at the same relative pressure. This phenomena suggests that there may exist a strong interaction between the *n*-hexylamine molecules and the surface of the Kevlar® fibers. This seems to correlate to some extent with the ΔG^{sp} and I^{sp} values of other polar probes at infinite dilution (Tables VI–VIII).

Figure 5 illustrates the energy distribution

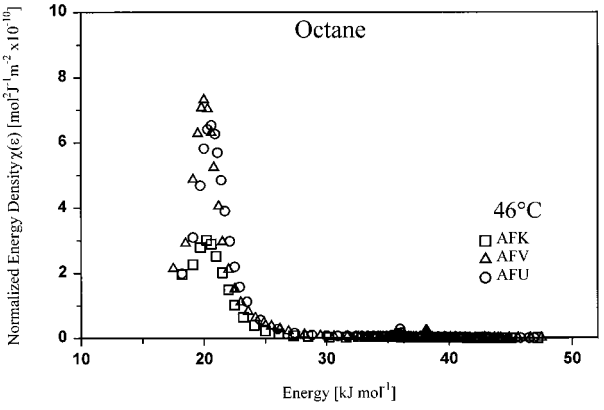

Figure 5 Energy distribution functions of the *n*-octane adsorption on Kevlar® fibers at 46°C.

function corresponding to the adsorption of *n*-octane on the fibers AFK, AFU, and AFV. The shape of the distribution profiles is almost the same for the three fibers. The peaks are relatively narrow with a sharp maximum around 20 kJ mol^{-1}. This agrees well with the free energy of adsorption measured at infinite dilution ($\sim$ 22 kJ mol^{-1} for *n*-octane; Table IV) and also indicates that the surface is quite homogeneous in terms of the energy site distribution. The peak height, representing the greatest concentration of energy sites, is relatively lower for the fiber AFK than for the larger diameter fibers AFU and AFV.

The energy distribution functions for the adsorption of *n*-hexylamine on the Kevlar® fiber samples are presented in Figure 6. It is quite astonishing to observe that the energy density distribution profiles for all fibers exhibit a very broad distribution on the high energy side, i.e., an unusual long peak tailing. An amazing binodal energy distribution appears with a main high energy concentration peak at 23 kJ mol^{-1} and another peak appearing as a shoulder around the energy value of 27 kJ mol^{-1}. These features are very reproducible. Several measurements have confirmed this result. The appearance of two peaks with a significant shoulder in the energy distribution profile may suggest the existence of two categories of energy sites on the fiber surface.

It is clear that the energy distribution functions, corresponding to the adsorption of *n*-octane and *n*-hexylamine on Kevlar® fibers, are quite different. As shown in Figure 6, the apparent peak broadening and shifting towards the higher energies related to the adsorption of *n*-hexylamine may indicate a strong specific interaction between the *n*-hexylamine molecules and the fiber surface.

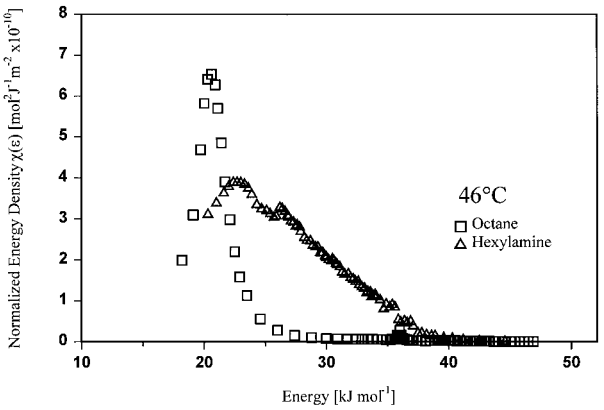

Figure 7 Comparison of the energy distribution functions between the adsorption of *n*-octane and *n*-hexylamine on the fiber AFU at 46°C.

Figure 7 reveals that the Kevlar® fiber surface becomes energetically heterogeneous with regard to the *n*-hexylamine, which is the opposite for the *n*-octane adsorption.

Comparison Between the Fiber Samples

From the above-described IGC results, the following differences have been found between the ultraclean fiber samples: higher γ_s^d values for AFV than AFK and AFU (Table V); equally higher ΔH_A°, ΔG_A°, and $\Delta G^{sp}/I^{sp}$ values for AFV (Tables III, IV, VI–VIII); a lower energy density for AFK in the case of the *n*-octane adsorption (Fig. 5); and a higher energy density for AFU in the case of *n*-hexylamine adsorption (Fig. 6). These differences certainly exist but could have been expected to be more significant. In reexamining the experimental conditions, one could consider that the column preconditioning temperature (180°C, 12 h) may cause a leveling off of the potential differences. A recent article gives the interesting indication on the heat treatment effect of [28] PPTA-based fibers. Lee et al.[28] showed that a heat treatment between 150 and 225°C for a short while (<10 s) modifies several properties of the Kevlar® fiber, such as tensile modulus, crystallite size, and orientation. However, these changes depend strongly on the applied axial tension, while the heating without tension has a much less effect.[28] Furthermore, it seems that the main property evolution occurs rapidly and reaches a stable value in less than 1 s for a given temperature and loading.[28] Our IGC column was stabilized in a moderately high temperature and a long time without axial tension being applied. However, surface structure evolution during the column conditioning could not be excluded. A recent communication[9] supports an annealing effect around 100–130°C on Kevlar® fibers. The authors observed with dodecane a discontinuity, around 100°C, of the straight line in a $\ln(Vn)$ versus $1/T$ plot comparable to Figure 3. In the case of free-length annealing, the adsorption enthalpy decreases from 99 kJ mol^{-1} for $T < 100$°C to 70 kJ mol^{-1} for $T > 120$°C. Apparently, the Kevlar®-29 fibers are also sensitive to the annealing at lower temperature (~ 100°C). In fact, an extrapolation to the dodecane probe of the ΔH_A° values given in Table III yields enthalpies in the range of 65–69 kJ mol, agreeing well with the observation of the other authors.[7,9] From the above discussion, it seems that the originally unannealed fibers AFK and AFV will be more influenced than the already annealed AFU fiber, although it appears logical that the smaller diameter and lower linear density of AFK could be considered as an intermediate sample due to its higher sensitivity to the drying heat and the column preconditioning at 180°C.

CONCLUSIONS

Surface energy properties have been studied using two IGC methods on three poly(*p*-phenylene terephthalamide) fibers (Kevlar®), at both infinite probe dilution and finite concentration. The results show the usefulness of this technique. At infinite dilution, two different calculation methods give consistent dispersive energy component γ_s^d values. The same magnitude of enthalpies for the alkane liquefaction and their adsorption on the fiber surfaces shows that the nonpolar probe molecules exchange similar interactions between them and the Kevlar® fiber surface. The specific interaction parameter for the polar probes, studied via three different data treatments, reveals the polar feature of the fiber surface, in good accordance with the observations using aniline as a polar probe.[10] This polar character is complemented well by the results at finite concentration. The *n*-hexylamine polar probe shows a higher affinity of adsorption than *n*-octane on the fiber surfaces. Furthermore, it is possible to map these surfaces in terms of their respective energy level distributions, which, according to the energy density function $\chi(\varepsilon)$, are energetically broad and heterogeneous for the *n*-hexylamine versus sharp and homogeneous for the *n*-octane. The energy

mapping illustrated in the present work might offer tremendous potential for the specific prevision of fiber to matrix compatibility in the area of polymer blends and composites, in which scientific enthusiasm seems to go well along with the industry challenges. On the other side, the lack of important differences between the various fiber families, also partly predictable, opens new avenues for the scientific investigation of heat memory effects on advanced fibers.

REFERENCES

1. H. Ishida, Ed., *Proceedings of the International Conference on Composite Interfaces,* Elsevier, Amsterdam, 1986.
2. L. T. Drzal, J. A. Meschen, and D. L. Hall, *Carbon,* **17,** 375 (1979).
3. E. Papirer and H. Balard, in *Acid–Base Interactions: Relevance to Adhesion Science and Technology,* K. D. Mittal and H. R. Anderson Jr., Eds., VSP BV, Utrech, The Netherlands, 1991, p. 191.
4. B. Rand and R. Robinson, *Carbon,* **15,** 311 (1977).
5. D. R. Lloyd, T. C. Ward, H. P. Schreiber, and C. C. Pizana, in *Inverse Gas Chromatography: Characterization of Polymers and other Materials,* D. R. Lloyd, T. C. Ward, and H. P. Schreiber, Eds., ACS Symposium Series 391, Washington, DC, 1989.
6. P. Mukhopadhyay and H. P. Schreiber, *Colloids and Surfaces,* **100,** 76 (1995).
7. A. S. Gozdz and H. D. Weigmann, *J. Appl. Polym. Sci.,* **29,** 3965 (1984).
8. P. J. C. Chappell and D. R. Williams, *J. Colloid Interface Sci.,* **128,** 450 (1989).
9. S. Rebouillat, M. Escoubes, R. Gauthier, and A. Vigier, *Polymer,* **36,** 4521 (1995).
10. S. Rebouillat, M. Escoubes, R. Gautier, and A. Vigier, *J. Appl. Polym. Sci.,* **58,** 1305 (1995).
11. J. R. Conder and C. L. Young, *Physicochemical Measurements by Chromatography,* John Wiley & Sons, New York, 1979.
12. M. J. Wang, S. Wolff, and J. B. Donnet, *Rubber Chem. Technol.,* **64,** 559 (1991).
13. S. Katz and D. G. Gray, *J. Colloid Interface Sci.,* **82,** 318 (1981).
14. J. H. De Boer, *The Dynamical Character of Adsorption,* Oxford University Press, London, 1953.
15. F. M. Fowkes, *Ind. Eng. Chem.,* **56,** 40 (1964).
16. G. M. Dorris and D. G. Gray, *J. Colloid Interface Sci.,* **77,** 353 (1980).
17. D. G. Le Grand and G. L. Gaines Jr., *J. Colloid Interface Sci.,* **31,** 162 (1963).
18. J. Schultz, L. Lavielle, and C. Martin, *J. Adhesion,* **23,** 45 (1987).
19. D. M. Young and A. D. Crowell, *Physical Adsorption of Gases,* Butterworths, London, 1962, p. 226.
20. J. B. Donnet, R. Y. Qin, and M. J. Wang, *J. Colloid Interface Sci.,* **153,** 572 (1992).
21. S. Dong, M. Brendlé, and J. B. Donnet, *Chromatographia,* **28,** 469 (1989).
22. W. T. Cooper and J. M. Hayes, *J. Chromatogr.,* **314,** 111 (1984).
23. R. Y. Qin and J. B. Donnet, *Carbon,* **32,** 165 (1994).
24. W. Rudzinski and D. H. Everett, *Adsorption of Gases on Heterogeneous Surface,* Academic Press, London, 1992.
25. W. Rudzinski, A. Waskmundzki, R. Leboda, and Z. Suptynowicz, *J. Chromatogr.,* **92,** 25 (1974).
26. J. P. Robson, *Can. J. Phys.,* **43,** 1941 (1965).
27. K. Haraguchi, T. Kajiyama, and M. Takayanagi, *J. Appl. Polym. Sci.,* **23,** 915 (1979).
28. K. G. Lee, R. Barton Jr., and J. M. Schultz, *J. Polym. Sci.,* **33,** 1 (1995).
29. S. Rebouillat, W. Huesch, J. B. Rappaport, personal communications.